Influence of Growth Temperature on TiO_2 Nanostructures by Hydrothermal Synthesis

Norazlina Ahmad, Fariza Mohamad, Mohd Khairul Ahmad, Azman Talib

Abstract*: Titanium dioxide (TiO2) shows a great interest in solar cell application due to its morphology and crystalline structure. Moreover, it is an affordable compound that could make solar cells more economical than traditional silicon solar cells. In this study, one-step hydrothermal method is demonstrated to synthesis TiO_2 nanorods/nanoflowers morphology on different hydrothermal reaction temperature. Increasing the reaction temperature could influence the formation of highly crystalline rutile phase of titania thin film. Moreover, the growth mechanism under different reaction temperatures has pronounced effects on the preferred orientation, morphologies and sizes of the structure. The results serve as guidance principle in preparing high quality solar cell specifically in heterojunction thin film fabrications.

***Index Terms*: Growth temperature, hydrothermal synthesis, thin film solar cell, TiO_2 nanorods/nanoflowers**

I. INTRODUCTION

TiO_2 is a one type of semiconductor material that attract many researchers to do the extensive study and substantial of literature had been produced for the past few decades regarding on its properties, functionality and the potential in industries application. There are thirteen polymorphs known of TiO_2 [1] but only three phases has widely been investigated namely anatase [2], [3], rutile [4], [5] and brookite [6], [7]. The anatase and rutile phases have a tetragonal structure whereas brookite is in orthorhombic phase. Rutile denotes as a steady phase at high temperatures and it is the apparent one to be realized as thin films or pure crystals. Anatase and brookite are meta-stable at all temperatures that upon heat treatment transform into rutile phase [8], [9].

Up to date, the interest towards TiO_2 nanostructures become popular because of its outstanding features for instances the large surface area exposable more to sunlight, high surface-to-volume ratio, non-toxicity, uniquely photochemical and photo-physical properties and also for their electron-transport properties [3]. The superior properties of nano TiO_2 are owing to its low dimensionality and quantum size effect [10] and because of these, it is essential to control the particle size, shape, and distribution of TiO_2 film.

A tremendous investigation has been conducted for the desired and controllable nanostructure including sol-gel process [11], [12], hydrothermal [13]–[15], chemical bath deposition [16], [17], spray pyrolysis [18]–[20] and anodization [21], [22]. Among these methods, hydrothermal is a promising approach and could be considered as convenient and feasible method [23], [24] in controlling the crystalline phase, grain size, morphology and surface chemistry by regulating the duration synthesis, reaction temperature, pressure, solution composition, solvent properties, additives and ageing time.

Li and co-workers investigated the effect of precursor concentration, hydrothermal reaction time and temperature in preparing TiO_2 nanorod arrays by hydrothermal method to control the morphologies and alignment of the nanostructure [25]. They claimed that at a high temperature, the density of the structure will enlarge and improve the orientation of nanorods growth. Furthermore, increasing the temperature and reaction duration of hydrothermal can promote the length and diameter of nanorods as well.

Liu & Aydil outlined seven factors including the effect of temperature, growth time, substrate type, acidity, reactant, concentration and precursors in their research that influenced the hydrothermally growth of nanorods structure [26]. They found that at temperature 200°C, the nanorods diameter decreased and the film partially lifted on the substrate due to the dissolution of the solution that reached an equilibrium state. Zhang and team employed a various temperature on synthesis TiO_2 buffer layer to improve the crystal quality of ZnO film [27]. They claimed that high temperature will reduce the stress of the intrinsic defect of the ZnO film. Srimala & Wei explained the effect of sodium hydroxide (NaOH) to TiO_2 ratio, reaction temperature, reaction time and annealing temperature on the formation of nanotubes structure synthesized by hydrothermal method [28]. They claimed that increasing the reaction temperature affected to the TiO_2 phase transformation and morphological properties.

In this article, one-step hydrothermal method is demonstrated to synthesis TiO_2 nanorods/nanoflowers morphology and the effect of the different reaction temperature has been studied and discussed. It shows that the growth mechanism under

Revised Manuscript Received on 14 September, 2019.

Norazlina Ahmad, Department of Electronic Engineering, Microelectronics and Nanotechnology Shamsuddin Research Centre (Mint-SRC), Universiti Tun Hussein Onn Malaysia, Batu Pahat, Johor, Malaysia. email address: azlina78.ahmad@gmail.com

Fariza Mohamad, Department of Electronic Engineering, Microelectronics and Nanotechnology Shamsuddin Research Centre (Mint-SRC), Universiti Tun Hussein Onn Malaysia, Batu Pahat, Johor, Malaysia.

Mohd Khairul Ahmad, Department of Electronic Engineering, Microelectronics and Nanotechnology Shamsuddin Research Centre (Mint-SRC), Universiti Tun Hussein Onn Malaysia, Batu Pahat, Johor, Malaysia.

Azman Talib, Department of Electronic Engineering, Microelectronics and Nanotechnology Shamsuddin Research Centre (Mint-SRC), Universiti Tun Hussein Onn Malaysia, Batu Pahat, Johor, Malaysia.

different temperatures has significant influences on the crystalline, orientation plane, morphologies and sizes of the structure synthesized.

II. MATERIALS AND METHOD

A. Preparation of TiO_2 nanorods/nanflowers

All the chemicals were analytically graded and used without further purification. Fluorine-doped SnO_2 (FTO) glass (7Ω/sq) with a thickness of 2.0mm was cut into the pieces of 1.5cm × 2.5cm in dimension as substrates. These substrates were cleaned ultrasonically in acetone, ethanol and de-ionized water (18.2MΩ, Mili-Q Ultrapure) in sequential for 10 minutes, respectively. In a typical synthesis, 80mL deionized water and 80mL concentrated hydrochloric acid (36.5%–38% by weight) stirring for 5 minutes before a desired amount of titanium butoxide (TBOT) was added drop by drop wisely using capillary tube and stirring for another 10 minutes until a clear mixed solution was obtained [29]. Then, the solution was relocated into a 300ml Teflon-lined stainless steel autoclave where the FTO substrates were horizontally placed with the conductive side facing upward and then the autoclave was sealed completely for hydrothermal synthesis in the oven. After cooling down to ambient temperature, the substrates were taken out, rinsed extensively with deionized water and allowed to dry naturally in ambient air. The prepared samples are denoted as '*GT-i*'; GT is referred as a growth temperature and '*-i*' is the value of temperature used.

B. Characterization Techniques

The crystal structure of the as-synthesized films was analyzed by Bruker D8 Advance X-ray diffraction (XRD) with CuKα radiation (λ) 1.5406 Å in the Bragg angle ranging from 20° to 70° at a scanning speed of $2°min^{-1}$ and the type of slit used was fixed divergence slit. X-ray tube voltage and current were set at 40kV and 40mA, respectively. The morphology and nanostructure of the samples were examined by field emission scanning electron microscopy (FE-SEM, JOEL, JSM-7600F). Element composition was identified by an energy dispersive X-ray spectroscope (EDS Oxford Instrument Inc.) incorporated to the FESEM. The absorbance spectra were recorded in a range of 300nm - 800nm on a UV–Vis–NIR spectrophotometer (Shimadzu-UV 1800) to find the wavelength absorption. Four-terminal sensing measurement known as 4Point Probe (Signatone Pro4-440N) connected to source meter to determine the resistivity properties of the samples.

III. RESULTS AND DISCUSSION

A. Structural Analysis

The X-ray diffraction pattern of the synthesized TiO_2 samples carried out at hydrothermal growth temperature 130°C, 150°C and 170°C are shown in Fig. 1. The obtained XRD patterns are compared with the standard JCPDS file no: 77-0452 for tetragonal rutile TiO_2 polymorphs and confirmed in line with tetragonal crustal structure space group $P4_2/mnm$. It is observed that at lower temperature, the strongest intense peak is corresponding to (101) plane. However, as elevating the temperature, the prominent peak has been changed to (110) plane as presented by samples GT150 and GT170. It is known that the rutile phase corresponding to (110) plane as the most exposed plane and generally obtained in many research work due on its thermodynamically stable at high temperature [30]. With the increasing of the temperature, the peak for rutile phase is significantly increased in intensity with the transformation of plane occurred as the growth is primarily formed at the {111} and {101} facets build up. One possible reason of this transformation is the order of surface energy E(110) < E(100) < E(101) < E(001) [31]. Also known as periodic bond chain (PBC), this order proposes a fast growing plane with high surface energy inclines to vanish and parting away a slower growing planes that having a lesser surface energy.

The diffraction rutile peaks observed for the sample GT130 at 2θ are 36.03°, 41° and 54.5° that attribute to (101), (111) and (211) planes respectively. It can be predicted by referring to the periodic bond chain, the {111} plane has a higher surface energy compared to {101} plane that promotes the initial growth of TiO_2 nanostructures on (111) and (211), followed by the growth on (101) plane. As the growth temperature increases to 150°C that represented as GT150, four peaks of rutile are detected with a new emergence of crystal growth on (110) plane corresponding to 2θ = 27.51° while the other peaks are resemble as GT130 sample but significantly change in intensity and crystallization. GT150 shows a prominent peak on (110) plane due on sharp and strong peak indicates high crystalline of TiO_2 film synthesized. As the temperature is elevated to 170°C, a sample denoted as GT170 exhibits the strongest peak at 2θ = 27.41° indexed to (110) plane.

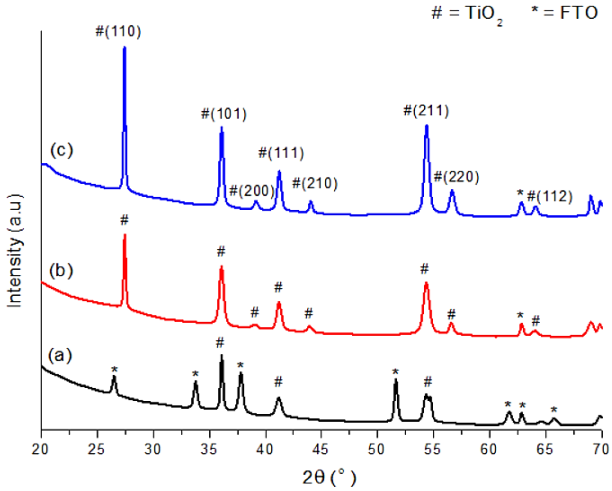

Fig. 1. XRD diffraction patterns of (a) GT130, (b) GT150 and (c) GT170 TiO_2 thin film.

The calculated crystallographic criterions of the as-prepared samples obtained are depicted in Table I. The Scherer equation has been adapted to calculate the crystallite size. The Scherer equation is given by

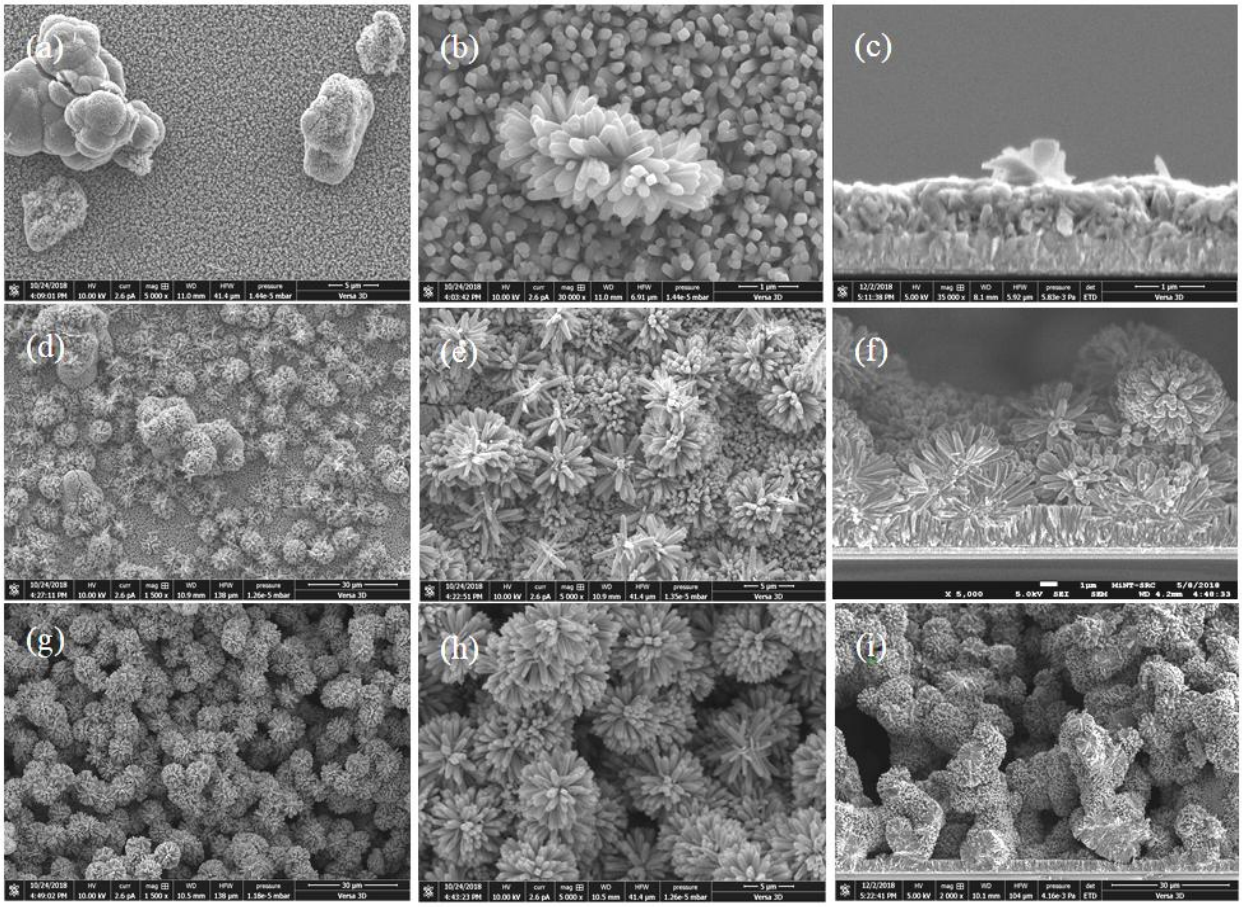

Fig. 2. FESEM surface morphologies of the samples (a), (b) GT130, (c), (d) GT150 and (e), (f) GT170 at different magnifications and (c), (f), (i) cross-section images, respectively.

$$D = \frac{K\lambda}{\beta \cos\theta} \quad (1)$$

where D is the crystal size; λ is the wavelength of the X-ray radiation (λ=0.15406 nm) for CuKα; K is constant and usually taken as 0.9; β is the line width at half-maximum height and θ is half of the diffraction angle (rad). The crystallite sizes obtained are 24.24nm, 69.27nm and 64.05nm corresponded to samples GT130, GT150 and GT170, respectively. The result exhibits improvement as increasing the growth temperature could improve the crystallite size of the samples.

From this work, it could evidently suggest that the temperature has a significant influence on the crystallite size of TiO_2. It can be elucidated that the plane transformation from (101) to (110) had been occurred when growth temperature is increased. Moreover, the crystallite size shows a significant improvement at moderate and higher temperature which is 150℃ and 170℃.

Table I: Structural criterions calculated from XRD patterns

Sample	*2θ (°)*	*β*	*Crystallite size, D (nm)*	*Plane, (hkl)*
GT130	36.03	0.3936	24.24	101
GT150	27.51	0.1476	69.27	110
GT170	27.41	0.2460	64.05	110

B. Surface Morphological

The morphology of TiO_2 thin films are observed with the FESEM images as shown in Fig. 2. The FESEM images revealed that TiO_2 nanorods had grown uniformly on the entire surface of FTO substrate, whereas the TiO_2 nanoflowers composed of nanorods was started to form on the nanorods when the initial growth temperature was 130℃. It was clearly seen that the TiO_2 nanoflowers were mono-sparse with low exposure on TiO_2 nanorods layer. The top of the surface of nanorods are tetragonal in shape with square top facets whereas the side surface are quite smooth and the nanoflowers have a pyramidal shape like tip indicate the general behaviour of rutile TiO_2 formation. The approximate diameter of TiO_2 nanorods was found to be 140nm while the nanoflower is found within the range of 140 – 180nm.

By elevating the temperature to 150℃, the hydrolysis rate was rapidly increased and enhanced the TiO_2 nanorods and nanoflowers growth. During the reaction, TiO_2 nanorods become elongated and nanoflowers are grown densely and randomly covered on the nanorods layer accordance to the surface energy level facet ranking. Also, the diameter of the nanorods increased and the nanoflowers structure has densely grown with many step-edges at the top of their petals with diameter ranging from 300 to 400nm.

Increasing the temperature to 170°C, the lengthy of nanorods is increased and more dense nanoflowers could be obtained, consistent with the result reported by Meidan Ye et al. [32]. The nanorods structure could not be seen anymore because the nanoflowers were too compact and fully covered on the nanorods layer. The top surface of the nanoflowers possessed of enormously step edges served as seed layer for the subsequent TiO_2 growth. The diameter of nanoflowers is significantly increased around 0.5µm. At higher temperature of 170°C, the nanoflowers growth becomes bigger than the TiO_2 nanoflowers at 150°C and 130°C. The nanoflowers thickness is increasing as the growth temperature is rising. The approximate thicknesses of the samples prepared at 130°C, 150°C and 170°C are 1.272µm, 9.28µm and up to 70µm, respectively.

From the EDS analysis, the sample GT130 shows the element composition of oxygen (O) 77.9%, titanium (Ti) element 15.91% and tin (Sn) element 6.19% as depicted in Table II. The result is confirmed with the XRD result that shows a presence of SnO structure on this sample. Increasing to the moderate temperature of sample GT150, the atomic elements of O is decreased to 66.31% but slightly increased to 33.69% for Ti element. Further rising the temperature as a sample GT170, the atomic are 65.06% of O and 34.94% of Ti. The oxygen content is slightly decreases as the growth temperature increases. This finding may attribute to the out-diffusion oxygen that occurred at moderate and high temperature [33]. No element of SnO is detected at moderate and high temperature slightly different from XRD result due to the compactness of TiO_2 nanorods/nanoflowers area during the EDS detection.

Table II. EDX data of the as-prepared samples

Sample	*Element (A= atomic %)*		
	Sn	O	Ti
GT130	A = 6.19	A = 77.90	A = 15.91
GT150	-	A = 66.31	A = 33.69
GT170	-	A = 65.06	A = 34.94

C. Optical Properties

Figure 3 illustrates the UV-vis diffuse reflectance spectrum of nanorods/nanoflowers TiO_2 structure of the prepared samples. The coefficient of optical absorbance of a semiconductor which near to the band edge can be articulated through the subsequent equation:

$$(h\upsilon\alpha)^n = A(h\upsilon - E_g) \qquad (2)$$

where $h\upsilon$ is the photon energy, α is the absorption coefficient, E_g is the absorption band gap, A is constant, n depends on the nature of the transitions, and may have values ½, 2, 2/3 and 3 corresponding to allowed indirect, allowed direct, forbidden direct and forbidden indirect transitions of band gap respectively. In this case, n = ½ is chosen for indirect allowed transition [33]. The absorption band edges were estimated around 400 nm slightly higher than normally reported of λ = 388 nm TiO_2.

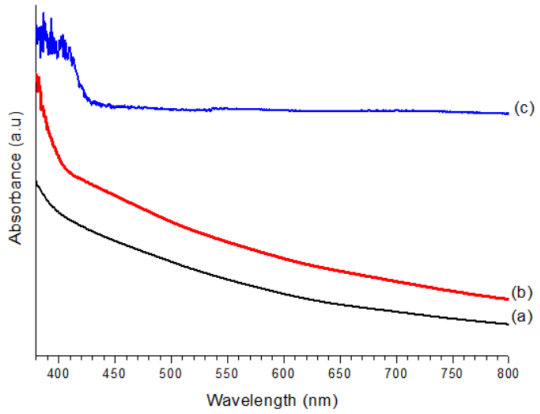

Fig. 3. UV-vis spectra of the TiO_2 samples (a) GT130, (b) GT150 and (c) GT170 TiO_2 thin film.

The intercept of the tangent to the plot $(\alpha h\upsilon)^{1/2}$ versus $h\upsilon$ as has been evaluated by Tauc plot equation to give an upright estimation of the band gap energy for this indirect band gap material. The indirect band gap energies (E_g) of as-prepared TiO_2 film are found to be 2.87eV, 2.83eV and 2.60eV for sample synthesis at 130°C, 150°C and 170°C as shown in Fig. 4. It elucidates the decreasing behaviour of TiO_2 band gap nanostructures as the growth temperature increasing. Therefore, it can be concluded that rising the growth temperature leads to the decreases of band gap energy of the prepared samples. This finding may attribute to a higher crystallite size of TiO_2 sample at higher temperature [34], [35].

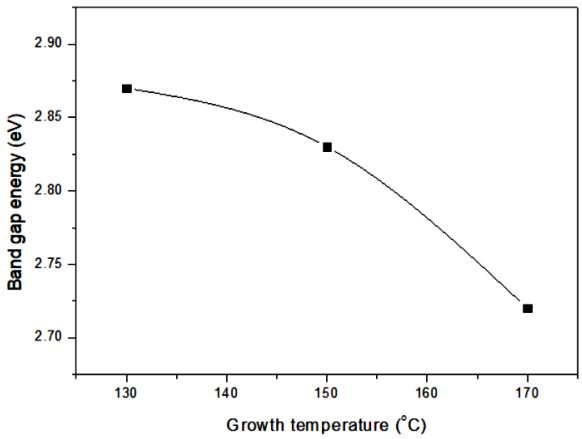

Fig. 4: Band gap of samples GT130, GT150 and GT170.

D. Electrical Properties

I-V analysis was carried out to measure the electrical properties of the TiO_2 thin film by using 4-point probe and the resistivity of the samples were obtained by the equation:

$$R_s = \frac{\rho}{t} \qquad (3)$$

where R_s is sheet resistance, ρ is resistivity and t is the thickness of the growth film and the result are depicted in Fig. 5.

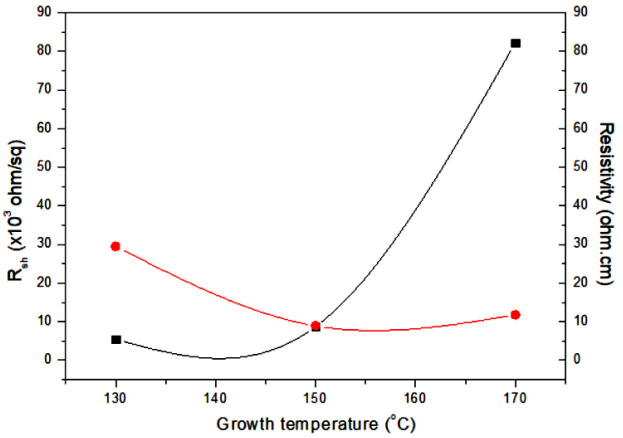

Fig. 5. Electrical properties of as-prepared samples synthesized at different growth temperatures.

It is clearly observed that the resistivity, ρ increases at high growth temperature that attributed to the thicker structure of TiO_2 film. Meanwhile, the sheet resistance shows the lowest values at the moderate temperature but increases at low and high temperature. It could be suggested that a very thin thickness of thin film is not suitable for electron transportation. The thickness of sample GT170 is excessively thick that deriving to high resistance. Therefore, an appropriate thickness is needed as it could provide enough channels for the electron to transfer, decrease the electron recombination nevertheless should not be in highly resistive.

IV. CONCLUSION

TiO_2 film has been successfully fabricated by one-step hydrothermal method on FTO glass substrate under various hydrothermal reaction temperatures as a crucial factor in hydrothermal process. It reveals that the growth of well-aligned rod-like layer is derived by tetragonal structure with small lattice mismatch between TiO_2 and FTO. Meanwhile, the formation of flower-like structure is due to the open space chemical reaction of the solution and encompasses the rod-like layer. Low temperature results an incomplete synthesis of thin film. Rising the temperature increasing the rod-like and compactness of the flower-like structures, simultaneously increases the thickness and resistivity of thin film. Therefore, this work suggested that moderate temperature is an adequate parameter for hydrothermally grown TiO_2 nanorods/nanoflowers layer. The results obtained show an optimum characteristic and regarded as a suitable candidate for heterojunction thin film formation.

ACKNOWLEDGMENT

This research work was supported by Program Hadiah Latihan Persekutuan 2017/2018, funded by Ministry of Education Malaysia, Microelectronic and Nanotechnology – Shamsuddin Research Centre (MiNT-SRC) and Universiti Tun Hussein Onn Malaysia (UTHM) for the facilities and chemicals provided as well the colleagues and expertise from technical support team.

REFERENCES

1. Q. J. Liu, Z. Ran, F. S. Liu, and Z. T. Liu, "Phase transitions and mechanical stability of TiO_2 polymorphs under high pressure," *J. Alloys Compd.*, vol. 631, pp. 192–201, 2015.
2. F. M. Hossain, A. V. Evteev, I. V. Belova, J. Nowotny, and G. E. Murch, "Electronic and optical properties of anatase TiO_2 nanotubes," *Comput. Mater. Sci.*, vol. 48, no. 4, pp. 854–858, 2010.
3. V. Dhas *et al.*, "Enhanced DSSC performance with high surface area thin anatase TiO_2 nanoleaves," *Sol. Energy*, vol. 85, no. 6, pp. 1213–1219, 2011.
4. L. Francis, A. Sreekumaran Nair, R. Jose, S. Ramakrishna, V. Thavasi, and E. Marsano, "Fabrication and characterization of dye-sensitized solar cells from rutile nanofibers and nanorods," *Energy*, vol. 36, no. 1, pp. 627–632, 2011.
5. Y. Li, M. Guo, M. Zhang, and X. Wang, "Hydrothermal synthesis and characterization of TiO_2 nanorod arrays on glass substrates," *Mater. Res. Bull.*, vol. 44, no. 6, pp. 1232–1237, 2009.
6. Ü. Ö. A. Arier and F. Z. Tepehan, "Controlling the particle size of nanobrookite TiO_2 thin film," *J. Alloys Compd.*, vol. 509, no. 32, pp. 8262–8267, 2011.
7. Y. Zou, X. Tan, T. Yu, Y. Li, Q. Shang, and W. Wang, "Synthesis and photocatalytic activity of chrysanthemum-like brookite TiO_2 nanostructures," *Mater. Lett.*, vol. 132, pp. 182–185, 2014.
8. B. Zhou, X. Jiang, Z. Liu, R. Shen, and A. V. Rogachev, "Preparation and characterization of TiO_2 thin film by thermal oxidation of sputtered Ti film," *Mater. Sci. Semicond. Process.*, vol. 16, no. 2, pp. 513–519, 2013.
9. L. Xu *et al.*, "Strong ultraviolet and violet emissions from ZnO/TiO_2 multilayer thin films," *Opt. Mater. (Amst).*, vol. 35, no. 8, pp. 1582–1586, 2013.
10. Y. Wang, Y. He, Q. Lai, and M. Fan, "Review of the progress in preparing nano TiO_2: An important environmental engineering material," *J. Environ. Sci.*, vol. 26, no. 11, pp. 2139–2177, 2014.
11. Ming Zhang, Y. Bando, and K. Wada, "Sol-gel template preparation of TiO_2 nanotubes and nanorods," *J. Mater. Sci. Lett.*, vol. 20, no. 2, pp. 167–170, 2001.
12. N. Venkatachalam, M. Palanichamy, and V. Murugesan, "Sol-gel preparation and characterization of nanosize TiO_2: Its photocatalytic performance," *Mater. Chem. Phys.*, vol. 104, no. 2–3, pp. 454–459, 2007.
13. W. Qi *et al.*, "Hydrothermal synthesis of TiO_2 nanorods arrays on ITO," *Mater. Chem. Phys.*, vol. 207, pp. 435–441, 2018.
14. R. Yoshida, Y. Suzuki, and S. Yoshikawa, "Syntheses of TiO_2(B) nanowires and TiO_2 anatase nanowires by hydrothermal and post-heat treatments," *J. Solid State Chem.*, vol. 178, no. 7, pp. 2179–2185, 2005.
15. S. Zanganeh *et al.*, "Hydrothermal synthesis and characterization of TiO_2 nanostructures using LiOH as a solvent," *Adv. Powder Technol.*, vol. 22, no. 3, pp. 336–339, 2011.
16. T. Dhandayuthapani, R. Sivakumar, and R. Ilangovan, "Growth of micro flower rutile TiO_2 films by chemical bath deposition technique: Study on the properties of structural, surface morphological, vibrational, optical and compositional," *Surfaces and Interfaces*, vol. 4, pp. 59–68, 2016.
17. A. Dussan, A. Bohórquez, and H. P. Quiroz, "Effect of annealing process in TiO_2 thin films: Structural, morphological, and optical properties," *Appl. Surf. Sci.*, vol. 424, pp. 111–114, 2017.
18. H. P. Deshmukh, P. S. Shinde, and P. S. Patil, "Structural, optical and electrical characterization of spray-deposited TiO_2 thin films," *Mater. Sci. Eng. B*, vol. 130, no. 1–3, pp. 220–227, 2006.
19. R. Manoharan, C and Sridhar, "Physical Properties of Spray Pyrolysed TiO2 Films," *Int. J. Recent Sci. Res.*, vol. 3, no. 9, pp. 775–777, 2012.
20. C. M. Firdaus, M. S. B. Shah Rizam, M. Rusop, and S. Rahmatul Hidayah, "Characterization of ZnO and ZnO: TiO_2 thin films prepared by sol-gel spray-spin coating technique," *Procedia Eng.*, vol. 41, no. Iris, pp. 1367–1373, 2012.
21. S. T. Nishanthi, S. Iyyapushpam, B. Sundarakannan, E. Subramanian, and D. Pathinettam Padiyan, "Inter-relationship between extent of anatase crystalline phase and photocatalytic activity of TiO_2 nanotubes prepared by anodization and annealing method," *Sep. Purif. Technol.*, vol. 131, pp. 102–107, 2014.
22. A. Tighineanu, T. Ruff, S. Albu, R. Hahn, and P. Schmuki, "Conductivity of TiO_2 nanotubes: Influence of annealing time and temperature," *Chem. Phys. Lett.*, vol. 494, no. 4–6, pp. 260–263, 2010.

23. H. Wang, G. Yi, M. Tan, X. Zu, H. Luo, and X. Jiang, "Initial reactant controlled synthesis of double layered TiO_2 nanostructures and characterization of its spectra of absorption and photoluminescence," *Mater. Lett.*, vol. 148, pp. 5–8, 2015.
24. H. Wang *et al.*, "A high-sensitive ultraviolet photodetector composed of double-layered TiO_2 nanostructure and Au nanoparticles film based on Schottky junction," *Mater. Chem. Phys.*, vol. 194, pp. 42–48, 2017.
25. L. Yuxiang, Z. Mei, G. Min, and W. Xidong, "Hydrothermal growth of well-aligned TiO_2 nanorod arrays: Dependence of morphology upon hydrothermal reaction conditions," *Rare Met.*, vol. 29, no. 3, pp. 286–291, 2010.
26. B. Liu and E. S. Aydil, "Growth of oriented single-crystalline rutile TiO_2 nanorods on transparent conducting substrates for dye-sensitized solar cells," *J. Am. Chem. Soc.*, vol. 131, no. 11, pp. 3985–3990, 2009.
27. W. Zhang, J. Zhao, Z. Liu, Z. Liu, and Z. Fu, "Influence of growth temperature of TiO_2 buffer on structure and PL properties of ZnO films," *Appl. Surf. Sci.*, vol. 256, no. 14, pp. 4423–4425, 2010.
28. S. Sreekantan and L. C. Wei, "Study on the formation and photocatalytic activity of titanate nanotubes synthesized via hydrothermal method," *J. Alloys Compd.*, vol. 490, no. 1–2, pp. 436–442, 2010.
29. M. K. Ahmad *et al.*, "Effect of heat treatment to the rutile based dye sensitized solar cell," *Optik (Stuttg).*, vol. 127, no. 8, pp. 4076–4079, 2016.
30. G.L. Li and G.H.Wang, "Synthesis and characterization of rutile TiO_2 nanowhiskers," *J. Mater. Res.*, pp. 3197–3206, 1998.
31. J. Lin *et al.*, "3D hierarchical rutile TiO_2 and metal-free organic sensitizer producing dye-sensitized solar cells 8.6% conversion efficiency," *Sci. Rep.*, vol. 4, pp. 1–8, 2014.
32. M. Ye, H. Y. Liu, C. Lin, and Z. Lin, "Hierarchical rutile TiO_2 flower cluster-based high efficiency dye-sensitized solar cells via direct hydrothermal growth on conducting substrates," *Small*, vol. 9, no. 2, pp. 312–321, 2013.
33. A. C. Khot *et al.*, "Bipolar resistive switching and memristive properties of hydrothermally synthesized TiO_2 nanorod array: Effect of growth temperature," *Mater. Des.*, vol. 151, pp. 37–47, 2018.
34. M. A. S. Maria John, K. Ramamurthi, K. Sethuraman, and R. Ramesh Babu, "Morphologically tuned 3D/1D rutile TiO_2 hierarchical hybrid microarchitectures engineered by one-step surfactant free hydrothermal method," *Appl. Surf. Sci.*, vol. 405, pp. 195–204, 2017.
35. V. V. Burungale *et al.*, "Studies on effect of temperature on synthesis of hierarchical TiO_2 nanostructures by surfactant free single step hydrothermal route and its photoelectrochemical characterizations," *J. Colloid Interface Sci.*, vol. 470, pp. 108–116, 2016.

AUTHOR PROFILE

I am **Norazlina Ahmad**, I am affiliated with Department of Electronic Engineering, Microelectronics and Nanotechnology Shamsuddin Research Centre (Mint-SRC), Universiti Tun Hussein Onn Malaysia, Batu Pahat, Johor, Malaysia. email address: azlina78.ahmad@gmail.com

I ma **Fariza Mohamad**, currently I am affiliated with Department of Electronic Engineering, Microelectronics and Nanotechnology Shamsuddin Research Centre (Mint-SRC), Universiti Tun Hussein Onn Malaysia, Batu Pahat, Johor, Malaysia.

I ma **Mohd Khairul Ahmad**, I ma associated with Department of Electronic Engineering, Microelectronics and Nanotechnology Shamsuddin Research Centre (Mint-SRC), Universiti Tun Hussein Onn Malaysia, Batu Pahat, Johor, Malaysia.

I ma **Azman Talib**, currently I am affiliated with Department of Electronic Engineering, Microelectronics and Nanotechnology Shamsuddin Research Centre (Mint-SRC), Universiti Tun Hussein Onn Malaysia, Batu Pahat, Johor, Malaysia.